

ISOGEOMETRIC PRECONDITIONERS BASED ON FAST SOLVERS FOR THE SYLVESTER EQUATION*

GIANCARLO SANGALLI[†] AND MATTIA TANI[†]

Abstract. We consider large linear systems arising from the isogeometric discretization of the Poisson problem on a single-patch domain. The numerical solution of such systems is considered a challenging task, particularly when the degree of the splines employed as basis functions is high. We consider a preconditioning strategy which is based on the solution of a Sylvester-like equation at each step of an iterative solver. We show that this strategy, which fully exploits the tensor structure that underlie isogeometric problems, is robust with respect to both mesh size and spline degree, although it may suffer from the presence of complicated geometry or coefficients. We consider two popular solvers for the Sylvester equation, a direct one and an iterative one, and we discuss in detail their implementation and efficiency for 2D and 3D problems. Numerical experiments for problems with different domain geometries are presented, which demonstrate the potential of this approach.

Key words. Isogeometric analysis, preconditioning, Kronecker product, Sylvester equation.

AMS subject classifications. 65N30, 65F08, 65F30

1. Introduction. The Isogeometric method is a computational technique for solving partial differential equations (PDEs). It has proposed in the seminal paper [23] as an extension of the classical finite element method, and is based on the idea of using splines or other functions constructed from splines (e.g., non-uniform rational B-splines, NURBS) both for the parametrization of the computational domain, as it is typically done by computer aided design software, and for the representation of the unknown solution fields of the PDE of interest. Many papers have demonstrated the effective advantage of isogeometric methods in various frameworks. The interested reader may find a detailed presentation of this idea with engineering applications in the book [10].

Unlike standard finite element methods, the isogeometric method makes possible to use high-regularity functions. The so-called isogeometric k -method, based on splines of degree p and global C^{p-1} regularity, has shown significant advantages in term of higher accuracy per degree-of-freedom in comparison to C^0 finite elements of degree p [11, 4]. However, the computational cost per degree-of-freedom is also higher for the k -method, in currently available isogeometric codes. In practice, quadratic or cubic splines are typically preferred as they maximise computational efficiency.

Standard isogeometric codes typically re-use finite element technology, which is very convenient but at the same time not the best choice for computational efficiency. The two fundamental stages of a linear PDE solver are the formation of the system matrix \mathcal{A} and the solution of the linear system $\mathcal{A}u = b$, and both stages, in standard isogeometric software, show a computational cost that grows significantly as the degree p grows. The focus of this paper is on the second stage, that is the linear solver.

The study of the computational efficiency of linear solvers for isogeometric discretizations has been initiated in the papers [9, 8], where it has been shown that the algorithms used with the finite element method suffer of performance degradation when used to solve isogeometric linear systems. Consider, for example, a Lagrangian finite element method with polynomial degree p and N degrees-of-freedom, in 3D: the

*Version of February 4, 2016

[†]Università di Pavia, Dipartimento di Matematica “F. Casorati”, Via A. Ferrata 1, 27100 Pavia, Italy. Emails: {sangia05,mattia.tani}@unipv.it

linear system matrix \mathcal{A} has a storage cost of $O(Np^3)$ non-zero terms and a solving cost by a direct solver of $O(N^2)$ floating point operations (FLOPs), (see [9, Section 2.3], under the assumption $N > p^6$). If, instead, we consider the isogeometric k -method with C^{p-1} p -degree splines and N degrees-of-freedom, still the linear system matrix \mathcal{A} has $O(Np^3)$ non-zero entries but a standard direct solver costs $O(N^2p^3)$ FLOPs, i.e., p^3 times more than a finite element approximation.

Iterative solvers have attracted more attention in the isogeometric community. The effort has been primarily on the development of preconditioners for the Poisson model problem, for arbitrary degree and continuity splines. As reported in [8], standard algebraic preconditioners (Jacobi, SSOR, incomplete factorization) commonly adopted for finite elements exhibit reduced performance when used in the context of the isogeometric k -method. Multilevel and multigrid approaches are studied respectively in [7] and [18], while advances in the theory of domain-decomposition based solvers are given in, e.g., [12, 5, 6]. These papers also confirm the difficulty in achieving both *robustness* and computational *efficiency* for the high-degree k -method. In this context, we say that a preconditioner \mathcal{P} for the linear system $\mathcal{A}u = b$ is robust if the condition number $\kappa(\mathcal{P}^{-1}\mathcal{A})$ is bounded from above by a reasonably low number, independent of the degree or continuity of the spline space adopted in the isogeometric discretization; we say that a preconditioner is computationally efficient if its setup and application has a computational cost comparable to the one of the matrix-vector product for the system matrix \mathcal{A} , i.e. $O(Np^3)$.

Robust multigrid preconditioners have been proposed in the recent papers [15] and [22]. The two works ground on the following common ingredients: first, in order to guarantee robustness, they rely on specific spectral properties of the discrete operator of the isogeometric k -method; second, they exploit the tensor-product structure of isogeometric spaces in order to achieve efficiency in multidimensional problems.

In this paper we also exploit the tensor-product structure of multivariate spline space, on a different basis. We ground on approaches that have been developed for the so-called Sylvester equation.

Consider the Laplace operator with constant coefficients, on the square $[0, 1]^2$, then the tensor-product spline Galerkin discretization leads to the system

$$(K_1 \otimes M_2 + M_1 \otimes K_2)u = b \quad (1.1)$$

where K_ℓ and M_ℓ denote the univariate stiffness and mass matrices in the ℓ direction, $\ell = 1, 2$, and \otimes is the Kronecker product. Equation (1.1), when reformulated as a matrix equation, takes the name of (generalized) Sylvester equation. This is a well studied problem in the numerical linear algebra literature, as it appears in many applications, e.g. stochastic PDEs, control theory, etc. (see the recent survey [32]). Observe that in general, for variable coefficients, general elliptic problems, non trivial and possibly multipatch geometry parametrization, the isogeometric system is not as in (1.1). In this case, a fast solver for (1.1) plays the role of a preconditioner. Having this motivation in mind, our aim is to study how the linear solvers for the Sylvester equation perform for (1.1), especially when originated by an isogeometric k -method.

We select two among the most popular algorithms: the first is the direct solver proposed by Bartels and Stewart in [2], the second is the alternating direction implicit (ADI) iterative solver, first introduced in [30] and further developed in a number of papers, among which [35]. The potential of ADI in the context of isogeometric problems has already been recognized in [19].

Our ultimate goal is the solution of 3D isogeometric systems, especially when high resolution is needed. A remarkable example is the simulation of turbulence,

see e.g. [3]. On a unit cube, still considering the Poisson problem, thanks to the tensor-product structure the linear system to solve takes the form

$$(K_1 \otimes M_2 \otimes M_3 + M_1 \otimes K_2 \otimes M_3 + M_1 \otimes M_2 \otimes K_3)u = b.$$

We hence consider extensions of Bartels-Stewart and ADI methods which can efficiently solve such problems.

We analyse and benchmark the proposed approaches in both 2D and 3D cases. Regarding computational efficiency, the Bartels-Stewart method exceed by far ADI. This is seen in 2D, but the gap is much wider in 3D. In 3D, the Bartels-Stewart solver count is $O(N^{4/3})$ FLOPs. ADI costs $O(Np)$ FLOPs per iteration, which result in an asymptotically lower operation counting. However, when used as a preconditioner in benchmarks that are representative of realistic problems, the Bartels-Stewart solver performs orders of magnitude better. In fact, in all our benchmarks that uses a conjugate gradient (CG) iterative solver, the computational time spent in the Bartels-Stewart preconditioner application is even lower than the residual computation (multiplication matrix \mathcal{A} times a vector). This surprising performance is due to the fact that the Bartels-Stewart solver requires dense matrix-matrix operations that takes advantages of modern computer architecture. In particular, the performance boost is due to the efficient use of the CPU hierarchy cache and memory access. Furthermore, the Bartels-Stewart method is especially suited to parallelisation which may significantly speed up the execution time, though this is not considered in our analysis.

For what concern robustness, both approaches are equivalent. The condition number $\kappa(\mathcal{P}^{-1}\mathcal{A})$ depends on the geometry parametrization of the computational domain Ω and of the coefficients of the differential operator. In this paper we study this dependence and perform some numerical tests. We will show that a singular mapping causes a loss of robustness, while $\kappa(\mathcal{P}^{-1}\mathcal{A})$ is uniformly bounded with respect to the degree p and mesh size h when the parametrization is regular. In all cases, it is important to have strategies to further improve the condition number, but this goes beyond the scope of the present work and we will the topic of further researches.

The outline of the paper is as follows. In Section 2 we introduce the matrices stemming from isogeometric discretization; we also recall the Kronecker product notation and its main properties. In Section 3 we define the preconditioner and discuss the spectral condition number of the preconditioned system. Sections 4 and 5 describe how such preconditioner can be efficiently applied in the 2D and 3D case, respectively. Numerical experiments are reported in Section 6. Finally, in Section 7 we draw the conclusions and outline future research directions.

2. Preliminaries.

2.1. Splines-based isogeometric method. We consider, as a model problem, the Poisson equation with Dirichlet boundary conditions:

$$\begin{cases} -\operatorname{div}(K(\mathbf{x})\nabla u(\mathbf{x})) = f(\mathbf{x}) & \text{on } \Omega \\ u = 0 & \text{on } \partial\Omega \end{cases} \quad (2.1)$$

where $K(\mathbf{x})$ is a symmetric positive definite matrix for each $\mathbf{x} \in \Omega$. In isogeometric methods, Ω is given by a spline or NURBS parametrization. For the sake of simplicity, we consider a single-patch spline parametrization.

Given two positive integers p and m , we say that $\Xi := \{\xi_1, \dots, \xi_{m+p+1}\}$ is an open knot vector if

$$\xi_1 = \dots = \xi_{p+1} < \xi_{p+2} \leq \dots \leq \xi_m < \xi_{m+1} = \dots = \xi_{m+p+1}, \quad (2.2)$$

where repeated knots are allowed, up to multiplicity p . Without loss of generality, we assume $\xi_1 = 0$ and $\xi_{m+p+1} = 1$. From the knot vector Ξ , B-spline functions of degree p are defined e.g. by the Cox-DeBoor recursive formula: piecewise constants ($p = 0$) B-splines are

$$\hat{B}_{i,0}(\zeta) = \begin{cases} 1 & \text{if } \xi_i \leq \zeta < \xi_{i+1}, \\ 0 & \text{otherwise,} \end{cases} \quad (2.3)$$

and for $p \geq 1$ the *B-spline* functions are obtained by the recursion

$$\hat{B}_{i,p}(\zeta) = \frac{\zeta - \xi_i}{\xi_{i+p} - \xi_i} \hat{B}_{i,p-1}(\zeta) + \frac{\xi_{i+p+1} - \zeta}{\xi_{i+p+1} - \xi_{i+1}} \hat{B}_{i+1,p-1}(\zeta), \quad (2.4)$$

where $0/0 = 0$. In general, the B-spline functions are degree p piecewise polynomial with $p - r$ continuous derivative at each knot with multiplicity r . In this work we are primarily interested in the so called *k-refinement* or *isogeometric k-method*, see [10]. For that, we assume the multiplicity of all internal knots is 1, which corresponds to C^{p-1} continuous splines. Each B-spline $\hat{B}_{i,p}$ depends only on $p + 2$ knots, which are collected in the *local knot vector*

$$\Xi_{i,p} := \{\xi_i, \dots, \xi_{i+p+1}\}.$$

When needed, we will adopt the notation $\hat{B}_{i,p}(\zeta) = \hat{B}[\Xi_{i,p}](\zeta)$. The support of each basis function is exactly $\text{supp}(\hat{B}_{i,p}) = [\xi_i, \xi_{i+p+1}]$.

Multivariate B-splines in dimension d ($d = 2, 3$ are the interesting cases) are defined from univariate B-splines by tensorization. For the sake of simplicity, we assume there are given a polynomial degree p and knot vectors $\Xi^\ell = \{\xi_{\ell,1}, \dots, \xi_{\ell,m+p+1}\}$, with the same length in all directions $\ell = 1, \dots, d$. Then for each multi-index $\mathbf{i} = (i_1, \dots, i_d)$, we introduce the local knot vector $\Xi_{i_1,p}^1 \times \dots \times \Xi_{i_d,p}^d$ and the multivariate B-spline

$$\hat{B}_{\mathbf{i},p}(\boldsymbol{\zeta}) = \hat{B}[\Xi_{i_1,p}^1](\zeta_1) \dots \hat{B}[\Xi_{i_d,p}^d](\zeta_d). \quad (2.5)$$

To simplify the notation, when not needed the subscript p is not indicated.

The domain Ω is given by a d -dimensional single-patch spline parametrization

$$\Omega = \mathbf{F}([0,1]^d), \text{ with } \mathbf{F}(\boldsymbol{\zeta}) = \sum_{\mathbf{i}} \mathbf{C}_{\mathbf{i}} \hat{B}_{\mathbf{i}}(\boldsymbol{\zeta}),$$

where $\mathbf{C}_{\mathbf{i}}$ are the control points. Following the isoparametric paradigm, the basis functions $B_{\mathbf{i}}$ on Ω are defined as $B_{\mathbf{i}} = \hat{B}_{\mathbf{i}} \circ \mathbf{F}^{-1}$. The isogeometric space, incorporating the homogeneous Dirichlet boundary condition, reads

$$V_h = \text{span}\{B_{\mathbf{i}} \text{ such that } \mathbf{i} = (i_1, \dots, i_d), \text{ with } 2 \leq i_\ell \leq m-1, 1 \leq \ell \leq d\} \quad (2.6)$$

We introduce a scalar indexing for functions in (2.6) as follows: to the each multi-index $\mathbf{i} = (i_1, \dots, i_d)$ we associate $i = 1 + \sum_{\ell=1}^d (m-2)^{\ell-1} (i_\ell - 2)$ and, with abuse of notation, indicate $B_{\mathbf{i}} = B_i$, etc. The dimension of V_h is denoted as $N = n^3$, where $n = m - 2$. Then, the Galerkin stiffness matrix reads

$$\begin{aligned} \mathcal{A}_{ij} &= \int_{\Omega} (\nabla B_i(\mathbf{x}))^T K(\mathbf{x}) \nabla B_j(\mathbf{x}) d\mathbf{x} \\ &= \int_{[0,1]^d} \left(\nabla \hat{B}_i(\boldsymbol{\xi}) \right)^T Q(\boldsymbol{\xi}) \nabla \hat{B}_j(\boldsymbol{\xi}) d\boldsymbol{\xi}, \quad i, j = 1, \dots, N \end{aligned} \quad (2.7)$$

where

$$Q = \det(J_{\mathbf{F}}) J_{\mathbf{F}}^{-T} K J_{\mathbf{F}}^{-1} \quad (2.8)$$

and $J_{\mathbf{F}}$ denotes the Jacobian of \mathbf{F} .

The support of a B-spline in V_h that does not touch $\partial\Omega$ intersects the support of $(2p+1)^d$ splines in V_h (including itself). If the support of a B-splines intersecting $\partial\Omega$, it overlaps at least $(p+1)^d$ and up to $(2p+1)^d$ B-spline supports (including itself). Thus, the number of nonzeros of \mathcal{A} is about $(2p+1)^d N$.

2.2. Kronecker product. Let $A \in \mathbb{R}^{n_a \times n_a}$, and $B \in \mathbb{R}^{n_b \times n_b}$. The *Kronecker product* between A and B is defined as

$$A \otimes B = \begin{bmatrix} a_{11}B & \dots & a_{1n_a}B \\ \vdots & \ddots & \vdots \\ a_{n_a1}B & \dots & a_{n_a n_a}B \end{bmatrix} \in \mathbb{R}^{n_a n_b \times n_a n_b}$$

where a_{ij} , $i, j = 1, \dots, n_a$, denote the entries of A . Kronecker product is an associative operation, and it is bilinear with respect to matrix sum and scalar multiplication. We now list a few properties of the Kronecker product that will be useful in the following sections.

- It holds

$$(A \otimes B)^T = A^T \otimes B^T. \quad (2.9)$$

- If C and D are matrices of conforming order, then

$$(A \otimes B)(C \otimes D) = (AC \otimes BD). \quad (2.10)$$

- If A and B are nonsingular, then

$$(A \otimes B)^{-1} = A^{-1} \otimes B^{-1}. \quad (2.11)$$

- If λ_i , $i = 1, \dots, n_a$, denote the eigenvalues of A and μ_j , $j = 1, \dots, n_b$, denote the eigenvalues of B , then the $n_a n_b$ eigenvalues of $A \otimes B$ have the form

$$\lambda_i \mu_j, \quad i = 1, \dots, n_a, \quad j = 1, \dots, n_b. \quad (2.12)$$

Property (2.9) implies that if A and B are both symmetric, then $A \otimes B$ is also symmetric. Moreover, if A and B are both positive definite, then according to (2.12) $A \otimes B$ is also positive definite.

For any matrix $X \in \mathbb{R}^{n_a \times n_b}$ we denote with $\text{vec}(X)$ the vector of $\mathbb{R}^{n_a n_b}$ obtained by “stacking” the columns of X . Then if A , B and X are matrices of conforming order, and $x = \text{vec}(X)$, it holds

$$(A \otimes B)x = \text{vec}(BXA^T) \quad (2.13)$$

This property can be used to cheaply compute matrix-vector products with a matrix having Kronecker structure. Indeed, it shows that computing $(A \otimes B)x$ is equivalent to computing n_b matrix-vector products with A and n_a matrix-vector products with B . Note in particular that $(A \otimes B)$ does not have to be formed.

If A and B are nonsingular, then (2.13) is equivalent to

$$(A \otimes B)^{-1}x = \text{vec}(A^{-1}XB^{-T}) \quad (2.14)$$

which, in a similar way, shows that the problem of solving a linear system having $(A \otimes B)$ as coefficient matrix is equivalent to solve n_b linear systems involving A and n_a linear systems involving B .

2.3. Evaluation of the computational cost and efficiency. Throughout the paper, we will primarily evaluate the computational cost of an algorithm by counting the number of floating point operations (FLOPs) it requires. A single addition, subtraction, multiplication or division performed in floating point arithmetic counts as one FLOP [20]. The number of FLOPs associated with an algorithm is an indication to assess its efficiency, and it is widely employed in literature. However, any comparison of FLOPs between different algorithms should be interpreted with caution. We emphasize, indeed, that the number of FLOPs represent just a portion of the computational effort required by an algorithm, as it does not take into account the movement of data in the memory and other overheads that affect the execution time. While these are difficult to estimate, we will discuss them when needed.

3. The preconditioner. Consider the matrix

$$\mathcal{P}_{ij} = \int_{[0,1]^d} \left(\nabla \hat{B}_i \right)^T \nabla \hat{B}_j d\xi, \quad i, j = 1, \dots, N \quad (3.1)$$

Observe that $\mathcal{P} = \mathcal{A}$ in the special case when K is the identity matrix and \mathbf{F} is the identity function, which means that $\Omega = [0, 1]^d$. For $d = 2$, by exploiting the tensor product structure of the basis functions we have

$$\mathcal{P} = K_1 \otimes M_2 + M_1 \otimes K_2$$

where M_1, M_2 represent the mass, and K_1, K_2 the stiffness univariate matrices.

$$(M_1)_{ij} = \int_0^1 \hat{B}[\Xi_i^1](\zeta_1) \hat{B}[\Xi_j^1](\zeta_1) d\zeta_1, \quad (M_2)_{ij} = \int_0^1 \hat{B}[\Xi_i^2](\zeta_2) \hat{B}[\Xi_j^2](\zeta_2) d\zeta_2,$$

$$(K_1)_{ij} = \int_0^1 (\hat{B}[\Xi_i^1])'(\zeta_1) \cdot (\hat{B}[\Xi_j^1])'(\zeta_1) d\zeta_1,$$

$$(K_2)_{ij} = \int_0^1 (\hat{B}[\Xi_i^2])'(\zeta_2) \cdot (\hat{B}[\Xi_j^2])'(\zeta_2) d\zeta_2.$$

Such matrices are all symmetric positive definite and banded with bandwidth p (we say that a matrix B has bandwidth p if $B_{ij} = 0$ for $|i - j| > p$). These matrices have the same order $n = m - 2$, where m is the dimension of the univariate spline space (see also from (2.2)). Similarly, when $d = 3$

$$\mathcal{P} = K_1 \otimes M_2 \otimes M_3 + M_1 \otimes K_2 \otimes M_3 + M_1 \otimes M_2 \otimes K_3.$$

By comparing (2.7) and (3.1), observe that $\mathcal{P}_{ij} \neq 0$ if and only if $\mathcal{A}_{ij} \neq 0$. Thus, despite having different entries in general, \mathcal{A} and \mathcal{P} have the same sparsity pattern.

We propose \mathcal{P} , defined in (3.1), as a preconditioner for the isogeometric matrix \mathcal{A} . In other words, we want to precondition a problem with arbitrary geometry and coefficients with a solver for the same operator on the parameter domain, with constant coefficients. This is a common approach, see e.g. [19], [15] and [22].

Note that, according to (2.9) and (2.12), \mathcal{P} is symmetric and positive definite, and hence we can use it as preconditioner for the conjugate gradient (CG) method. At each CG iteration, we need to solve a system of the form

$$\mathcal{P}s = r \quad (3.2)$$

where r is the current residual. Due to the structure of \mathcal{P} , (3.2) is a Sylvester-like equation. How to efficiently solve this system for $d = 2$ and $d = 3$, employing solvers for Sylvester equation, will be the topic of Sections 4 and 5. In this section we discuss the effects of geometry and coefficients on the overall CG convergence. The next proposition provides an upper bound for the spectral condition number of $\mathcal{P}^{-1}\mathcal{A}$.

PROPOSITION 1.

It holds

$$\kappa(\mathcal{P}^{-1}\mathcal{A}) \leq \frac{\sup_{\Omega} \lambda_{\max}(Q)}{\inf_{\Omega} \lambda_{\min}(Q)} \quad (3.3)$$

where the matrix Q is given in (2.8).

Proof.

Let $u = (u_1, \dots, u_N)^T \in \mathbb{R}^n$, and define $u_h = \sum_{i=1}^N u_i \hat{B}_i$. Then it holds

$$\begin{aligned} u^T \mathcal{A} u &= \int_{[0,1]^d} (\nabla u_h)^T Q \nabla u_h \, d\xi \leq \int_{[0,1]^d} \lambda_{\max}(Q) \|\nabla u_h\|^2 \, d\xi \\ &\leq \sup_{\Omega} \lambda_{\max}(Q) \int_{[0,1]^d} \|\nabla u_h\|^2 \, d\xi = \sup_{\Omega} \lambda_{\max}(Q) u^T \mathcal{P} u \end{aligned}$$

By the Courant-Fischer theorem, we infer $\lambda_{\max}(\mathcal{P}^{-1}\mathcal{A}) \leq \sup_{\Omega} \lambda_{\max}(Q)$. With analogous calculations one can show that $\lambda_{\min}(\mathcal{P}^{-1}\mathcal{A}) \geq \inf_{\Omega} \lambda_{\min}(Q(\xi))$, and hence

$$\kappa(\mathcal{P}^{-1}\mathcal{A}) \leq \frac{\sup_{\Omega} \lambda_{\max}(Q)}{\inf_{\Omega} \lambda_{\min}(Q)}.$$

□

Proposition 1 represents the formalization of an intuitive fact. As long as the considered problem doesn't depart much from the model problem on the square with constant coefficients, the right-hand side of (3.3) will be small and the preconditioner is expected to perform well. On the other hand, if the eigenvalues of Q vary widely, due to the presence of complicated geometry or coefficients, the preconditioner performance decreases. In these cases, it is useful to have strategies to improve the spectral conditioning of $\mathcal{P}^{-1}\mathcal{A}$: this is a topic that we will address in a forthcoming paper. We emphasize that bound (3.3) does not depend neither on the mesh size nor on the spline degree, but only on \mathbf{F} and K .

Furthermore Proposition 1 allows one to compare the strategies proposed in this paper with different approaches which do not rely on the preconditioner \mathcal{P} . This might be helpful not only from the theoretical point of view, but also from a practical perspective. Indeed, during the process of assembling the stiffness matrix \mathcal{A} , the matrix Q can be evaluated at all quadrature points of the mesh and the extreme eigenvalues of Q can be computed in order to estimate the right-hand side of (3.3). This leads to a reliable estimate of $\kappa(\mathcal{P}^{-1}\mathcal{A})$ before attempting to solve the system. If another solver is available, which does not suffer from complicated geometry or coefficients, then a smart software could use the estimate on $\kappa(\mathcal{P}^{-1}\mathcal{A})$ to automatically choose which method is more suited to solve the system at hand.

4. The 2D case. When $d = 2$, equation (3.2) takes the form

$$(K_1 \otimes M_2 + M_1 \otimes K_2) s = r \quad (4.1)$$

Using relation (2.13), we can rewrite this equation in matrix form

$$M_2SK_1 + K_2SM_1 = R \quad (4.2)$$

where $\text{vec}(S) = s$ and $\text{vec}(R) = r$. Equation (4.2) takes the name of (generalized) Sylvester equation. Due to its many applications, the literature dealing with Sylvester equation (and its variants) is vast, and a number of methods have been proposed for its numerical solution. We refer to [32] for a recent survey on this subject. In this paper, we consider two among the most studied methods, which in authors' perspective seem the most suited for the particular features of IGA problems. The Bartels-Stewart method is a direct solver, which means that $s = \mathcal{P}^{-1}r$ is computed exactly. The alternating direction implicit (ADI) method is an iterative solver, which means that s is computed only approximately. We remark that ADI was first applied to IGA problems in [19].

To keep the notation consistent with the rest of the paper, in this section we will favor the Kronecker formulation (4.1) with respect to the matrix equation form (4.2).

4.1. Bartels-Stewart direct method. We describe a direct method for (4.1) that was first presented in 1964 by Lynch, Rice and Thomas [28] as a method for solving elliptic partial differential equation discretized with finite differences. This approach was extended to a general Sylvester equation involving nonsymmetric matrices by Bartels and Stewart in 1972 [2]. Due to its popularity in the context of the Sylvester equation, we refer to this approach as the Bartels-Stewart method, despite focusing on its symmetric variant.

We consider the generalized eigendecomposition of the matrix pencils (K_1, M_1) and (K_2, M_2) , namely

$$K_1U_1 = M_1U_1D_1 \quad K_2U_2 = M_2U_2D_2 \quad (4.3)$$

where D_1 and D_2 are diagonal matrices whose entries are the eigenvalues of $M_1^{-1}K_1$ and $M_2^{-1}K_2$, respectively, while U_1 and U_2 satisfy

$$U_1^T M_1 U_1 = I, \quad U_2^T M_2 U_2 = I,$$

which implies in particular $U_1^{-T}U_1^{-1} = M_1$ and $U_2^{-T}U_2^{-1} = M_2$, and also, from (4.3), $U_1^{-T}D_1U_1^{-1} = K_1$ and $U_2^{-T}D_2U_2^{-1} = K_2$. Therefore we factorize \mathcal{P} in (4.1) as follows:

$$(U_1 \otimes U_2)^{-T} (D_1 \otimes I + I \otimes D_2) (U_1 \otimes U_2)^{-1} s = r,$$

and adopt the following strategy:

Algorithm 1 Bartels-Stewart direct method (symmetric case)

- 1: Compute the generalized eigendecompositions (4.3)
 - 2: Compute $\tilde{r} = (U_1 \otimes U_2)^T r$
 - 3: Compute $\tilde{s} = (D_1 \otimes I + I \otimes D_2)^{-1} \tilde{r}$
 - 4: Compute $s = (U_1 \otimes U_2) \tilde{s}$
-

Computational cost. The exact cost of the eigendecompositions in line 1 depends on the algorithm employed. We refer to [20, Chapter 8], [14, Section 5.3] and references therein for an overview of the state-of-the-art methods. A simple approach is to first compute the Cholesky factorization $M_1 = LL^T$ and the symmetric matrix

$\widetilde{K}_1 = L^{-T} K_1 L^{-1}$. Since M_1 and K_1 are banded, the cost of these computations is $O(pn^2)$ FLOPs. The eigenvalues of \widetilde{K}_1 are the same of (4.3), and once the matrix \widetilde{U}_1 of orthonormal eigenvectors is computed then one can compute $U_1 = L^{-1} \widetilde{U}_1$, again at the cost of $O(pn^2)$ FLOPs. Being \widetilde{U}_1 orthogonal, then $U_1^T M_1 U_1 = I_n$. If the eigendecomposition of \widetilde{K}_1 is computed using a divide-and-conquer method, the cost of this operation is roughly $4n^3$ FLOPs. We remark that the divide-and-conquer approach is also very suited for parallelisation. In conclusion, by this approach, line 1 requires roughly $8n^3$ FLOPs.

Lines 2 and 4 each involve a matrix-vector product with a matrix having Kronecker structure, and each step is equivalent (see (2.13)) to 2 matrix products involving dense $n \times n$ matrices. The total computational cost of both steps is $8n^3$ FLOPs. Line 3 is just a diagonal scaling, and its $O(n^2)$ cost is negligible. We emphasize that the overall computational cost of Algorithm 1 is independent of p .

If we apply Algorithm 1 as a preconditioner, then Step 1 may be performed only once, since the matrices involved do not change throughout the CG iteration. In this case the main cost can be quantified in approximately $8n^3$ FLOPs per CG iterations. The other main computational effort of each CG iteration is the residual computation, that is the product of the system matrix \mathcal{A} by a vector, whose cost in FLOPs is twice the number of nonzero entries of \mathcal{A} , that is approximately $2(2p+1)^2 n^2$. In conclusion, the cost ratio between the preconditioner application and the residual computation is about $4n/(2p+1)^2 \approx n/p^2$.

4.2. The ADI method. The ADI method was originally proposed in 1955 by Peaceman and Rachford as a method to solve elliptic and parabolic differential equations with two space variables [30] by a structured finite difference discretization. An important contribution to the early development of ADI is due to Wachspress and collaborators [34] [35] [27] [17]. In 1999, Penzl [31] proposed a low-rank version of ADI, which is suited to solve very large problems. In this paper, however, we will focus on the so-called “classical” ADI method and will not consider the low-rank variant. For more details on the classical ADI method, we refer to the monograph [37].

The j -th iteration of the ADI method applied to equation (4.1) reads:

$$((K_1 + \omega_j M_1) \otimes M_2) s_{j-1/2} = r - (M_1 \otimes (K_2 - \omega_k M_2)) s_{j-1} \quad (4.4a)$$

$$(M_1 \otimes (K_2 + \gamma_j M_2)) s_j = r - ((K_1 - \gamma_j M_1) \otimes M_2) s_{j-1/2} \quad (4.4b)$$

where $\gamma_j, \omega_j \in \mathbb{R}$ are acceleration parameters, which will be discussed in the next section. Note that at each ADI iteration we need to solve two linear systems where the coefficient matrix has a Kronecker product structure, which can be solved efficiently by (2.11).

4.2.1. Convergence analysis. Let s be the exact solution of the system $\mathcal{P}s = r$, then a straightforward computation yields

$$((K_1 + \omega_j M_1) \otimes M_2) s = r - (M_1 \otimes (K_2 - \omega_j M_2)) s \quad (4.5a)$$

$$(M_1 \otimes (K_2 + \gamma_j M_2)) s = r - ((K_1 - \gamma_j M_1) \otimes M_2) s \quad (4.5b)$$

If $e_j = s - s_j$ denotes the error at the j -th iteration, then by subtracting (4.5) to (4.4), we get

$$((K_1 + \omega_j M_1) \otimes M_2) e_{j-1/2} = - (M_1 \otimes (K_2 - \omega_j M_2)) e_{j-1} \quad (4.6a)$$

$$(M_1 \otimes (K_2 + \gamma_j M_2)) e_j = - ((K_1 - \gamma_j M_1) \otimes M_2) e_{j-1/2} \quad (4.6b)$$

from which we derive

$$e_j = M^{-1/2} \left[\left(\widetilde{K}_1 + \omega_j I \right)^{-1} \left(\widetilde{K}_1 - \gamma_j I \right) \otimes \left(\widetilde{K}_2 + \gamma_j I \right)^{-1} \left(\widetilde{K}_2 - \omega_j I \right) \right] M^{1/2} e_{j-1},$$

where $M = M_1 \otimes M_2$, $\widetilde{K}_1 = M_1^{-1/2} K_1 M_1^{-1/2}$ and $\widetilde{K}_2 = M_2^{-1/2} K_2 M_2^{-1/2}$.

If J denotes the total number of iterations, by recursive application of this formula we obtain

$$e_J = M^{-1/2} T_J M^{1/2} e_0 \quad (4.7)$$

where

$$T_J = \prod_{j=1}^J \left(\widetilde{K}_1 - \gamma_j I \right) \left(\widetilde{K}_1 + \omega_j I \right)^{-1} \otimes \left(\widetilde{K}_2 + \gamma_j I \right)^{-1} \left(\widetilde{K}_2 - \omega_j I \right) \quad (4.8)$$

Given a vector $v \in \mathbb{R}^N$, its M -norm is defined as

$$\|v\|_M := \sqrt{v^T M v}$$

Note that $\|v\|_M = \|M^{1/2} v\|$. With this definition, from (4.7) we infer that

$$\frac{\|e_J\|_M}{\|e_0\|_M} \leq \|T_J\|$$

We now observe that the factors of T_J , namely $\left(\widetilde{K}_1 + \omega_j I \right)^{-1} \left(\widetilde{K}_2 - \omega_j I \right)$ and $\left(\widetilde{K}_1 - \gamma_j I \right) \left(\widetilde{K}_2 + \gamma_j I \right)^{-1}$ for $j = 1, \dots, J$, are symmetric and all share the same set of orthonormal eigenvectors. As a consequence, T_J is symmetric and its eigenvalues are products of the eigenvalues of the factors. Hence,

$$\|T_J\| = \max_{\lambda \in \Lambda(M_1^{-1} K_1), \mu \in \Lambda(M_2^{-1} K_2)} \prod_{j=1}^J \left| \frac{\lambda - \gamma_j}{\lambda + \omega_j} \cdot \frac{\mu - \omega_j}{\mu + \gamma_j} \right|$$

If $\Lambda(M_1^{-1} K_1) \subseteq [a, b]$ and $\Lambda(M_2^{-1} K_2) \subseteq [c, d]$, we can bound the norm of T_J by replacing the maximum over the discrete spectra with the maximum over the continuous intervals, i.e.

$$\|T_J\| \leq \max_{\lambda \in [a, b], \mu \in [c, d]} \prod_{j=1}^J \left| \frac{\lambda - \gamma_j}{\lambda + \omega_j} \cdot \frac{\mu - \omega_j}{\mu + \gamma_j} \right|$$

Thus we are interested in choosing the parameters $\omega_j, \gamma_j, i = 1, \dots, J$ that solve the following minmax problem:

$$\rho_J := \min_{\omega_1, \dots, \omega_J, \gamma_1, \dots, \gamma_J} \left(\max_{\lambda \in [a, b], \mu \in [c, d]} \prod_{j=1}^J \left| \frac{\lambda - \gamma_j}{\lambda + \omega_j} \cdot \frac{\mu - \omega_j}{\mu + \gamma_j} \right| \right) \quad (4.9)$$

An explicit expression for such optimal parameters was first presented in [34] for the special case $[a, b] = [c, d]$ and $J = 2^t, t \in \mathbb{N}$, and then in [35] for the general case. In

order to simplify the analysis, for the rest of this section we will assume $[a, b] = [c, d]$ and take $\gamma_j = \omega_j$, $j = 1, \dots, J$.

When the optimal parameters are selected, the value of ρ_J in (4.9) can be expressed in terms of elliptic functions. However, it can be approximated (see [37, Chapter 1] for the technical details) as:

$$\rho_J \approx 4 \exp \left(-\frac{\pi^2 J}{\ln \left(4 \frac{b}{a} \right)} \right) \quad (4.10)$$

Assuming the the above relation is accurate (which is true in typical situations), then the number of ADI iterations needed to ensure $\|T_J\| \leq \epsilon$ is

$$J = \left\lceil \frac{1}{\pi^2} \ln \left(4 \frac{b}{a} \right) \ln \left(\frac{4}{\epsilon} \right) \right\rceil \quad (4.11)$$

where $\lceil \cdot \rceil$ denotes the integer round toward positive infinity. We emphasize that the dependence of J on the spectral condition number of the matrices involved is logarithmic, and hence extremely mild. Moreover, once a tolerance ϵ is chosen, the number of ADI iterations can be selected a priori according to (4.11).

4.2.2. The algorithm. A simple trick to reduce the computational cost of each ADI iteration is to define

$$\tilde{s}_i = \begin{cases} (M_1 \otimes I_n) s_i & \text{for } i \in \mathbb{N} \\ (I_n \otimes M_2) s_i & \text{for } i \notin \mathbb{N} \end{cases}$$

Equations (4.4) now read

$$\begin{aligned} ((K_1 + \omega_j M_1) \otimes I_n) \tilde{s}_{j-1/2} &= r - (I_n \otimes (K_2 - \omega_j M_2)) \tilde{s}_{j-1} \\ (I_n \otimes (K_2 + \gamma_j M_2)) \tilde{s}_j &= r - ((K_1 - \gamma_j M_1) \otimes I_n) \tilde{s}_{j-1/2} \end{aligned}$$

We now summarize the steps of the ADI method.

Algorithm 2 ADI method

- 1: Fix the number of iterations J according to (4.11)
 - 2: Compute the parameters ω_j , γ_j , $j = 1, \dots, J$.
 - 3: Set $\tilde{s}_0 = 0$.
 - 4: **for** $j = 1, \dots, J$ **do**
 - 5: Set $r_{j-1} = r - (I_n \otimes (K_2 - \omega_j M_2)) \tilde{s}_{j-1}$.
 - 6: Solve $((K_1 + \omega_j M_1) \otimes I_n) \tilde{s}_{j-1/2} = r_{j-1}$.
 - 7: Set $r_{j-1/2} = r - ((K_1 - \gamma_j M_1) \otimes I_n) \tilde{s}_{j-1/2}$.
 - 8: Solve $(I_n \otimes (K_2 + \gamma_j M_2)) \tilde{s}_j = r_{j-1/2}$.
 - 9: **end for**
 - 10: Set $s_J = (M_1 \otimes I_n)^{-1} \tilde{s}_J$.
-

4.2.3. ADI as a preconditioner. Our main interest is to apply ADI as a preconditioner. We observe that, if we take as initial guess $s_0 = 0$ then equality (4.7) can be rewritten as

$$s_J = M^{-1/2} (I - T_J) M^{1/2} \mathcal{P}^{-1} r =: \mathcal{P}_J^{-1} r$$

Hence performing J iterations of the ADI method to the system $\mathcal{P}s = r$ is equivalent to multiply r by the matrix $\mathcal{P}_J^{-1} = M^{-1/2} (I - T_J) M^{1/2} \mathcal{P}^{-1}$.

In order to apply ADI as a preconditioner for CG, two issues has to be addressed. First, the CG method may break down if an arbitrary preconditioner is considered; in order to safely use the ADI method, we need to show that \mathcal{P}_J is symmetric and positive definite. Second, the choice of the tolerance ϵ for ADI is crucial and has to be discussed. Indeed, a tolerance that is too strict yields unnecessary work, while a tolerance that is too loose may compromise the convergence of CG.

The following theorem addresses both issues. In particular, it presents a nice and simple upper bound for the spectral conditioning of $\mathcal{P}_J^{-1} \mathcal{A}$ in terms of ϵ and of the conditioning of the exactly preconditioned system $\mathcal{P}^{-1} \mathcal{A}$. A proof of this theorem, which generalizes the results of [35, Section 3], can be found in [37]. We give a proof of this theorem in our notation, to keep the present manuscript as self-contained as possible.

THEOREM 1.

The ADI preconditioner \mathcal{P}_J (with optimal parameters) is positive definite. Moreover, if $\|T_J\| \leq \epsilon$, then it holds

$$\kappa(\mathcal{P}_J^{-1} \mathcal{A}) \leq \left(\frac{1 + \epsilon}{1 - \epsilon} \right) \kappa(\mathcal{P}^{-1} \mathcal{A}) \quad (4.12)$$

Proof.

We note that \mathcal{P}_J is symmetric and positive definite if and only if the same holds true for

$$M^{1/2} \mathcal{P}_J^{-1} M^{1/2} = (I - T_J) \tilde{\mathcal{P}}^{-1}. \quad (4.13)$$

with $\tilde{\mathcal{P}} = M^{-1/2} \mathcal{P} M^{-1/2}$. We have already observed that T_J is symmetric. Moreover, $I - T_J$ is positive definite, since $\|T_J\| = \rho_J < 1$. The last inequality is apparent by considering the definition of ρ_J in (4.9); indeed if we take any set of parameters that satisfy $0 < \gamma_j, \omega_j \leq \min\{a, c\}$, $j = 1, \dots, J$, then each factor of the product is strictly smaller than 1.

We observe that $\tilde{\mathcal{P}} = \tilde{K}_1 \otimes I + I \otimes \tilde{K}_2$ and $I - T_J$ share the same set of eigenvectors, and since they are both symmetric and positive definite, the product in (4.13) is again symmetric and positive definite.

We now turn on inequality (4.12). Matrix $\mathcal{P}_J^{-1} \mathcal{A}$ is similar to

$$\tilde{\mathcal{P}}^{1/2} M^{1/2} \mathcal{P}_J^{-1} \mathcal{A} M^{-1/2} \tilde{\mathcal{P}}^{-1/2} = (I - T_J) \left(\tilde{\mathcal{P}}^{-1/2} M^{-1/2} \mathcal{A} M^{-1/2} \tilde{\mathcal{P}}^{-1/2} \right),$$

where we used the fact that $\tilde{\mathcal{P}}^{1/2}$ and $I - T_J$ commute, since they share the same set of eigenvectors.

It holds

$$\begin{aligned} \lambda_{\max}(\mathcal{P}_J^{-1} \mathcal{A}) &= \lambda_{\max} \left((I - T_J) \left(\tilde{\mathcal{P}}^{-1/2} M^{-1/2} \mathcal{A} M^{-1/2} \tilde{\mathcal{P}}^{-1/2} \right) \right) \\ &\leq \left\| (I - T_J) \left(\tilde{\mathcal{P}}^{-1/2} M^{-1/2} \mathcal{A} M^{-1/2} \tilde{\mathcal{P}}^{-1/2} \right) \right\| \\ &\leq \|I - T_J\| \cdot \left\| \tilde{\mathcal{P}}^{-1/2} M^{-1/2} \mathcal{A} M^{-1/2} \tilde{\mathcal{P}}^{-1/2} \right\| \\ &\leq (1 + \epsilon) \lambda_{\max} \left(\tilde{\mathcal{P}}^{-1/2} M^{-1/2} \mathcal{A} M^{-1/2} \tilde{\mathcal{P}}^{-1/2} \right) \\ &= (1 + \epsilon) \lambda_{\max}(\mathcal{P}^{-1} \mathcal{A}). \end{aligned} \quad (4.14)$$

$p = 1$	$p = 2$	$p = 3$	$p = 4$	$p = 5$	$p = 6$	$p = 7$	$p = 8$
$3 \cdot 10^5$	$3 \cdot 10^5$	$4 \cdot 10^5$	$4 \cdot 10^5$	$1 \cdot 10^6$	$2 \cdot 10^6$	$2 \cdot 10^6$	$3 \cdot 10^6$

TABLE 4.1
Spectral condition number of $M_1^{-1}K_1$, with $h = 2^{-5}$.

With analogous computations one can show that

$$\lambda_{\min}(\mathcal{P}_J^{-1}\mathcal{A}) \geq (1 - \epsilon) \lambda_{\min}(\mathcal{P}^{-1}\mathcal{A}) \quad (4.15)$$

Combining (4.15) and (4.14), inequality (4.12) is proved.

□

4.2.4. Computational cost. Lines 1 and 2 of Algorithm 2, namely the computation of J and of the optimal parameters, require an estimate of the minimum and maximum eigenvalue of $M_1^{-1}K_1$ and $M_2^{-1}K_2$. Since all the matrices involved are symmetric, positive definite and banded, this task can be achieved inexpensively, e.g. with a few iterations of the power method.

The computational effort of one full ADI iteration consists in $2n$ matrix-vector products (lines 5 and 7 of Algorithm 2) and the solution of $2n$ linear systems (lines 6 and 8), both of which involve banded matrices of order n . Since lines 5 and 7 also require a vector update of order n^2 , the total cost of a single ADI iteration is roughly $(16p + 10)n^2$ FLOPs.

The cost of a single iteration has to be multiplied for the number iterations J , given by (4.11), in order to obtain the total cost of ADI. For IGA mass and stiffness matrices, it holds $\frac{b}{a} = \kappa(M_1^{-1}K_1) \leq c_p h^{-2} \approx c_p n^2$, where c_p is a constant that depends only on p . From inverse estimates for polynomials it follows $c_p \leq p^4$, however no accurate estimate of c_p is known yet. Hence, we seek numerical evidence of the dependence of $\kappa(M_1^{-1}K_1)$ with respect to p . The results, obtained for $h = 2^{-5}$, are reported in Table 4.1. We can see that the growth of the conditioning is not dramatic, with a growth which is weaker than the bound above and, since we are only interested in its logarithm, we can conclude that the number of ADI iterations is robust with respect to p for the practical situation of interest.

In conclusion the total cost of ADI is roughly

$$\left[\frac{1}{\pi^2} \ln(4c_p n^2) \ln\left(\frac{4}{\epsilon}\right) + 1 \right] (16p + 10)n^2$$

FLOPs. We observe that the cost of the preconditioner is (almost) linear w.r.t. to the number of degrees of freedom, and very robust with respect to p . Indeed, this cost has a milder dependence on p than the cost of a matrix-vector product with \mathcal{A} , which is $2(2p + 1)^2 n^2$ FLOPs.

5. The 3D case. When $d = 3$, equation (3.2) takes the form

$$(K_1 \otimes M_2 \otimes M_3 + M_1 \otimes K_2 \otimes M_3 + M_1 \otimes M_2 \otimes K_3)s = r \quad (5.1)$$

As in the 2D case, we consider both a direct and an iterative method, which are generalizations of the approaches detailed in the previous section, namely the Bartels-Stewart method and the ADI method. Other possible approaches are then summarized.

5.1. The direct method. The direct method presented in section 4.1 admits a straightforward generalization to the 3D case (see also [26], where an analogous approach is considered for the nonsymmetric case). We consider the generalized eigendecompositions

$$K_1 U_1 = M_1 U_1 D_1, \quad K_2 U_2 = M_2 U_2 D_2, \quad K_3 U_3 = M_3 U_3 D_3 \quad (5.2)$$

with D_1, D_2, D_3 diagonal matrices and

$$U_1^T M_1 U_1 = I, \quad U_2^T M_2 U_2 = I, \quad U_3^T M_3 U_3 = I.$$

Then, (5.1) can be factorized as

$$(U_1 \otimes U_2 \otimes U_3)^{-1} (D_1 \otimes I \otimes I + I \otimes D_2 \otimes I + I \otimes I \otimes D_3) (U_1 \otimes U_2 \otimes U_3)^{-T} s = r,$$

which suggests the following algorithm.

Algorithm 3 3D Bartels-Stewart direct method

- 1: Compute the generalized eigendecompositions (5.2)
 - 2: Compute $\tilde{r} = (U_1 \otimes U_2 \otimes U_3)r$
 - 3: Compute $\tilde{s} = (D_1 \otimes I \otimes I + I \otimes D_2 \otimes I + I \otimes I \otimes D_3)^{-1} \tilde{r}$
 - 4: Compute $s = (U_1 \otimes U_2 \otimes U_3)^T \tilde{s}$
-

5.1.1. Computational cost. Lines 1 and 3 require $O(n^3)$ FLOPs. Lines 2 and 4, as can be seen by nested applications of formula (2.13), are equivalent to performing a total of 6 products between dense matrices of size $n \times n$ and $n \times n^2$. Thus, neglecting lower order terms the overall computational cost of Algorithm 3 is $12n^4$ FLOPs.

The direct method is even more appealing in the 3D case than it was in the 2D case, for at least two reasons. First, the computational cost associated with the preconditioner setup, that is the eigendecomposition, is negligible. This means that the main computational effort of the method consists in a few (dense) matrix-matrix products, which are level 3 BLAS operations and typically yield high efficiency thanks to a dedicated implementation on modern computers by optimised usage of the memory cache hierarchy [20, Chapter 1]. Matrix-matrix products are also naturally suited for parallelisation. Second, in a preconditioned CG iteration the cost for applying the preconditioner has to be compared with the cost of the residual computation (a matrix-vector product with \mathcal{A}) which can be quantified in approximately $2(2p+1)^3 n^3$ for 3D problems, resulting in a FLOPs ratio of the preconditioner application to residual computation (matrix-vector product) of $(3n)/(4p^3) \approx n/p^3$. For example, if $N = 256^3$ and $p = 4$, the preconditioner requires only 3 times more FLOPs than the residual computation, while for degree $p = 6$ the matrix-vector product is even more costly than the preconditioner itself. However in numerical tests we will see that, for all cases of practical interest in 3D, the computational time used by the preconditioner application is far lower than the residual computation itself. This is because the computational time depends not only on the FLOPs count but also on the memory usage and, as mentioned above, dense matrix-matrix multiplications greatly benefit of modern computer architecture. This approach will show largely higher performance than the alternative ADI approach we have considered.

5.2. Three-variable ADI. Despite the clear advantages presented by the direct method discussed in the previous section, for the sake of comparison we also consider ADI. Indeed ADI may benefit from a lower FLOPs counting than the direct solver, for large n and low p , and being an iterative solver we can optimise the target precision as needed by the preconditioning step.

However, the ADI extension to the 3D case is not straightforward. We follow the iterative scheme proposed by Douglas in [16] to solve (5.1):

$$(\mathcal{K}_1 + \omega_j M) s_{j-2/3} = 2r - (\mathcal{K}_1 + 2\mathcal{K}_2 + 2\mathcal{K}_3 - \omega_j M) s_{j-1} \quad (5.3a)$$

$$(\mathcal{K}_2 + \omega_j M) s_{j-1/3} = \mathcal{K}_2 s_{j-1} + \omega_j M s_{j-2/3} \quad (5.3b)$$

$$(\mathcal{K}_3 + \omega_j M) s_j = \mathcal{K}_3 s_{j-1} + \omega_j M s_{j-1/3} \quad (5.3c)$$

where $\mathcal{K}_1 = K_1 \otimes M_2 \otimes M_3$, $\mathcal{K}_2 = M_1 \otimes K_2 \otimes M_3$, $\mathcal{K}_3 = M_1 \otimes M_2 \otimes K_3$, $M = M_1 \otimes M_2 \otimes M_3$, and the ω_j are real positive parameters. After J steps, reasoning as in the 2D case, we can derive an expression for the error e_J similar to (4.7):

$$e_J = M^{-1/2} T_J M^{1/2} e_0,$$

where T_J is a symmetric positive definite matrix that depends on $\omega_1, \dots, \omega_J$. Hence, the relative error in the M -norm is bounded by the euclidean norm of T_J .

We assume for simplicity that $\Lambda(M_1^{-1}K_1) = \Lambda(M_2^{-1}K_2) = \Lambda(M_3^{-1}K_3) = [a, b]$. Then it can be shown that

$$\|T_J\| \leq \max_{\lambda_1, \lambda_2, \lambda_3 \in [a, b]} \left| \prod_{j=1}^J \left(1 - 2\omega_j^2 \frac{\lambda_1 + \lambda_2 + \lambda_3}{(\omega_j + \lambda_1)(\omega_j + \lambda_2)(\omega_j + \lambda_3)} \right) \right| =: \rho_J(\omega_1, \dots, \omega_J). \quad (5.4)$$

Clearly we are interested in choosing the parameters ω_j , $j = 1, \dots, J$ so that the function ρ_J is minimized. This minmax problem mirrors (4.9), but unlike that case, no expression for the solution is known. This means that for 3D ADI, we cannot rely on an optimal choice for the parameters; this makes the ADI approach less appealing than in the 2D case. The suboptimal choice proposed in [16] still guarantees that the number of iterations J_0 needed to ensure that $\|T_{J_0}\| \leq \epsilon$ satisfies

$$J_0 \approx 1.16 \ln \left(\frac{b}{a} \right) \ln(\epsilon^{-1}) = O \left(\ln \left(\frac{b}{a} \right) \ln(\epsilon^{-1}) \right), \quad (5.5)$$

Note that also in the 2D case we have that the number of iterations required to achieve convergence is $O(\ln(\frac{b}{a}) \ln(\epsilon^{-1}))$ (cf. (4.11)). However, in the 3D case the constant hidden in this asymptotic estimate is significantly greater than the one of the 2D case.

In fact, our numerical experience indicates that typically the condition $\|T_J\| \leq \epsilon$ is satisfied after much fewer iterations than (5.5) would suggest. To avoid unnecessary iterations, we introduce an a different stopping criterion, based on the evaluation of the right hand side of (5.3). More precisely, we compute the parameters $\omega_1, \dots, \omega_{J_0}$ according to [16] but then perform only the first $J \leq J_0$ iterations, where J is the smallest index such that $\rho_J(\omega_1, \dots, \omega_J) \leq \epsilon$.

To reduce the computational cost of one ADI iteration, we multiply the first equation of (5.3) by $(I_n \otimes M_2 \otimes M_3)^{-1}$, the second by $(M_1 \otimes I_n \otimes M_3)^{-1}$ and the third by $(M_1 \otimes M_2 \otimes I_n)^{-1}$. After some algebraic manipulation we obtain

$$\begin{aligned} ((K_1 + \omega_j M_1) \otimes I_n \otimes I_n) s_j^* &= \tilde{r} - ((K_1 - \omega_j M_1) \otimes I_n \otimes I_n) s_{j-1} - 2(M_1 \otimes I_n \otimes I_n) \\ &\quad \cdot (I_n \otimes M_2^{-1} K_2 \otimes I_n + I_n \otimes I_n \otimes M_3^{-1} K_3) s_{j-1} \end{aligned} \quad (5.6a)$$

$$\begin{aligned} (I_n \otimes (K_2 + \omega_j M_2) \otimes I_n) s_j^{**} &= (I_n \otimes M_2 \otimes I_n) \\ &\quad \cdot ((I_n \otimes M_2^{-1} K_2 \otimes I_n) s_{j-1} + \omega_j s_j^*) \end{aligned} \quad (5.6b)$$

$$\begin{aligned} (I_n \otimes I_n \otimes (K_3 + \omega_j M_3)) s_j &= (I_n \otimes I_n \otimes M_3) \\ &\quad \cdot ((I_n \otimes I_n \otimes M_3^{-1} K_3) s_{j-1} + \omega_j s_j^{**}) \end{aligned} \quad (5.6c)$$

where $\tilde{r} = 2(I_n \otimes M_2 \otimes M_3)^{-1} r$. Note that the vectors

$$u_j := (I_n \otimes M_2^{-1} K_2 \otimes I_n) s_{j-1}, v_j := (I_n \otimes I_n \otimes M_3^{-1} K_3) s_{j-1},$$

which both appear twice in (5.6), need to be computed only once. We consider one last trick to save some computational cost. Let

$$b_j := (I_n \otimes I_n \otimes M_3^{-1} K_3) s_{j-1} + \omega_j s_j^{**},$$

then

$$v_{j+1} = (I_n \otimes I_n \otimes M_3)^{-1} (I_n \otimes I_n \otimes (K_3 + \omega_j M_3)) s_j - \omega_j s_j = b_j - \omega_j s_j.$$

where the last equality is a consequence of equation (5.6c). Hence we can use the known vectors b_j and s_j to inexpensively compute v_{j+1} .

We summarize all these considerations in Algorithm 4.

Algorithm 4 3D ADI method

- 1: Compute all the eigenvalues of $M_1^{-1} K_1$, $M_2^{-1} K_2$ and $M_3^{-1} K_3$.
 - 2: Compute the number of iterations J and parameters $\omega_1, \dots, \omega_J$ such that $\rho_J(\omega_1, \dots, \omega_J) \leq \epsilon$.
 - 3: Compute $\tilde{r} = 2(I_n \otimes M_2 \otimes M_3)^{-1} r$.
 - 4: Set $s_0, v_0 = 0$.
 - 5: **for** $j = 1, \dots, J$ **do**
 - 6: Solve $(I_n \otimes M_2 \otimes I_n) u_j = (I_n \otimes K_2 \otimes I_n) s_{j-1}$
 - 7: Compute the right-hand side of (5.6a): $r_j^* = \tilde{r} - ((K_1 - \omega_j M_1) \otimes I_n \otimes I_n) s_{j-1} - (2M_1 \otimes I_n \otimes I_n) (u_j + v_j)$
 - 8: Solve $((K_1 + \omega_j M_1) \otimes I_n \otimes I_n) s_j^* = r_j^*$
 - 9: Compute the right-hand side of (5.6b): $r_j^{**} = (I_n \otimes M_2 \otimes I_n) (u_j + \omega_j s_j^*)$
 - 10: Solve $(I_n \otimes (K_2 + \omega_j M_2) \otimes I_n) s_j^{**} = r_j^{**}$
 - 11: Set $b_j = v_j + \omega_j s_j^{**}$
 - 12: Compute the right-hand side of (5.6c): $r_j = (I_n \otimes I_n \otimes M_3) b_j$
 - 13: Solve $(I_n \otimes I_n \otimes (K_3 + \omega_j M_3)) s_j = r_j$
 - 14: Set $v_{j+1} = b_j - \omega_j s_j$
 - 15: **end for**
-

As for the previous methods, we are mainly interested in using ADI as a preconditioner. It can be shown that Theorem 1 holds also in the 3D case. We do not report the details, as the arguments used in the proof are the same as in the 2D case. This means that the 3D ADI can be used as a preconditioner for CG and that relation (4.12) guides in choosing the inner tolerance ϵ .

5.2.1. Computational cost. At each iteration, the main computational effort is represented by the solution of four linear systems (lines 5, 7, 9 and 12) and five matrix products (lines 5, 6, 8, and 11). As always, by exploiting the Kronecker structure of the matrices involved, each of these computations can be performed at a cost of $2(2p+1)n^3$ FLOPs. A careful analysis reveals that the total cost of a single ADI iteration is $(36p+29)n^3$ FLOPs, where we neglected terms of order lower than n^3 .

Unlike in the 2D case, the number of iterations J is not known a priori. However, if we consider J_0 in (5.5) as an upper bound for the number of iterations, we can bound the total computational cost can be bounded roughly by

$$1.16 \ln(c_p n^2) \ln(\epsilon^{-1}) (36p+29) n^3. \quad (5.7)$$

where, as in the 2D case, we replaced $\frac{b}{a}$ with $c_p n^2$. We observe that asymptotically the complexity of ADI is almost $O(n^3)$, that is almost linear w.r.t. the number of degrees of freedom. On the other hand, a closer look at (5.7) reveals that the number of FLOPs required may actually very large, even for small or moderate p . The sequential nature of the ADI iteration makes it less suited for parallelisation than the direct method.

5.3. Other approaches. In this section, we briefly summarize two other approaches which approximately solves (5.1) while yielding linear complexity w.r.t. the number of degrees of freedom. We do not pursue these approaches further, as in our numerical experiments (see the next section) the direct method proved itself to be extremely efficient for all the discretization levels considered, despite its $O(n^4)$ complexity.

1. **Reduction to standard Sylvester equation.** By considering (2.13), equation (5.1) can be reformulated as

$$K_{23}SM_1 + M_{23}SM_1 = (M_2 \otimes K_3 + K_2 \otimes M_3)SM_1 + (M_2 \otimes M_3)SK_1 = R$$

where $s = \text{vec}(S)$, $r = \text{vec}(R)$ (cf. [29, Section 6.2]). This is a (generalized) Sylvester matrix equation having as coefficient matrices $K_{23}, M_{23} \in \mathbb{R}^{n^2 \times n^2}$ and $M_1, K_1 \in \mathbb{R}^{n \times n}$. If this equation is solved using the Bartels-Stewart method, the resulting approach is equivalent to applying Algorithm 3 to the original problem. On the other hand, if one attempts to solve this Sylvester equation with the standard ADI method, then at each iteration n linear systems with coefficient matrix $K_{23} + \gamma_j M_{23}$ have to be solved. This coefficient matrix is again sum of two Kronecker product, hence it can be solved approximately using an inner ADI iteration. This inner-outer ADI strategy, which is further discussed in [36] and [37, Section 2.3], yields an overall complexity $O(n^3)$ is achieved. As a drawback, even when a loose tolerance is required for the outer iteration, a strict tolerance has to be imposed on the inner iteration to ensure the overall convergence of the method.

2. **Low-rank approximation.** This approach consists in approximating the right-hand side of (5.1) as

$$r \approx \sum_{j=1}^t x_j \otimes y_j \otimes z_j, \quad x_j, y_j, z_j \in \mathbb{R}^n \quad (5.8)$$

where t is called the *rank* of the approximation, whose value may be fixed by the user or be adaptive. We refer to [24] and references therein for a discussion on low-rank approximation of tensors.

If we assume that a good enough low-rank approximation of r is available, then the Kronecker structure of the new right-hand side can be exploited in the solution of the tensor equation. We refer to the algorithms proposed in [21], [25] and [1].

6. Numerical experiments. We now numerically show the potential of the approaches described in Sections 4 and 5. All the algorithms are implemented in MATLAB Version 8.5.0.197613 (R2015a), with the toolbox GEOPDES [13], on a 12x Intel Xeon i7-5820K, 3.30GHz, 64 GB of RAM.

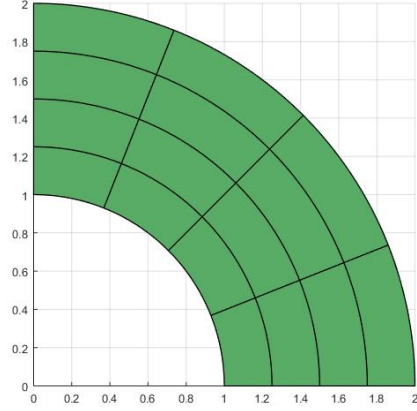
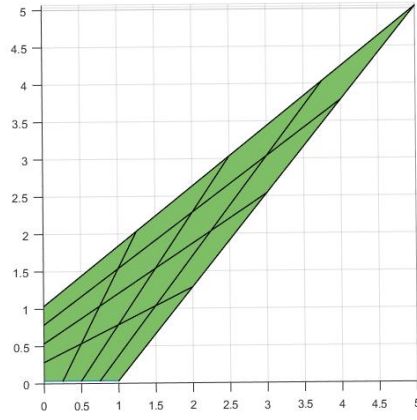
We give a few technical details on how the methods were implemented. For Bartels-Stewart method, we used the MATLAB function `eig` to compute the generalized eigendecomposition (4.3) and (5.2). For 2D ADI, the number of iterations was set according to (4.11). The extreme eigenvalues of $M_1^{-1}K_1$ and $M_2^{-1}K_2$, which are required for computing the optimal parameters derived in [35], were approximated using 10 iterations of the (direct and inverse) power method. For 3D ADI, the eigenvalue computation necessary to select the parameters was again performed using `eig`. In both 2D and 3D, at each ADI iteration the linear systems were solved using MATLAB's direct solver "backslash". Finally, in 3D algorithms the products involving Kronecker matrices were performed using the function from the free MATLAB toolbox Tensorlab [33]. We recall MATLAB allows implicit parallelism for some of its operations, e.g. dense matrix multiplication, `eig` and the direct solver.

Although in many of the problems considered here the matrix pencils (K_1, M_1) , (K_2, M_2) (and in the 3D case (K_3, M_3)) coincide, we never exploit this fact in our tests. For example, in line 1 of Algorithm 1 we always compute two eigendecompositions even if in the current problem we have $M_1 = M_2$ and $K_1 = K_2$. In this way, the computational effort reflects the more general case in which such matrices are different.

6.1. 2D experiments. We start by considering 2D problems, and observe the performance of the Bartels-Stewart and ADI methods on four test problems with different geometries: a square, a quarter of ring, a stretched square and plate with hole. In all problems we set K as the identity matrix, since according to Proposition 1 the presence of coefficients and of a nontrivial geometry have an analogous impact on the difficulty of the problem.

The square domain is simply $[0, 1]^2$. The quarter of ring is shown in Figure 6.1, the stretched square (which was considered also in [19]) is shown in Figure 6.2, and the plate with hole is shown in Figure 6.3. The last case deserves further comments. In the chosen parametrization, which is the same considered in [10, Section 4.2], two control points are placed in the same spacial location, namely the left upper corner, and this creates a singularity in the Jacobian of \mathbf{F} . In this case, the bound provided by Proposition 1 becomes $\kappa(\mathcal{P}^{-1}\mathcal{A}) \leq +\infty$, and it is hence useless. In principle, our approaches could perform arbitrarily bad and this problem is indeed intended to test their performance in this unfavorable case. In all problems, except the last one, the system $\mathcal{A}u = b$ represents the discretization of problem (2.1), with $f = 2(x^2 - x) + 2(y^2 - y)$. For the plate with hole domain, we considered $f = 0$ and mixed boundary conditions.

We start by considering the problem on the square. As already said, in this case $\mathcal{P} = \mathcal{A}$ and we can directly apply the considered method to the system $\mathcal{A}u = b$. This is not a realistic case but serves as a preliminary check on the proposed theory and implementations. Results are shown in Table 6.1; in the upper part we report the CPU time for Bartels-Stewart method, while in the lower part we report the number

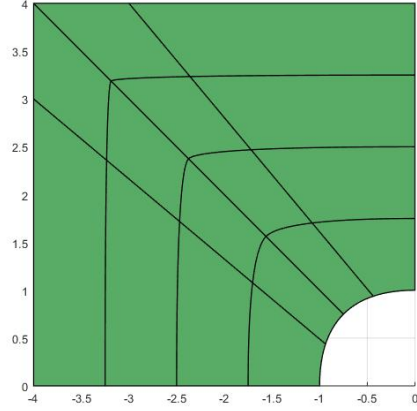
FIG. 6.1. *Quarter of ring domain*FIG. 6.2. *Stretched square domain*

of iterations and CPU time for ADI, whose tolerance was set to 10^{-8} , for different values of h and p .

We observe that the computation time for the direct method is substantially independent w.r.t. p ; fluctuations in time appearing in the finer discretization levels are due to the `eig` function, which constitute the main computational effort of the method in our implementation. For the ADI method, the computation time increases with p , although the dependence is mild.

Concerning the dependence on h , based on the analysis of computational cost we expect ADI to perform better than the direct method for small enough h . That is indeed what we can see in the experimental results, although only for an extremely small value of h , corresponding roughly to 64 millions degrees of freedom. However, we emphasize that the CPU times of the two methods are comparable for all the discretization levels considered.

The number of iterations of ADI is determined a priori, according to (4.11), and

FIG. 6.3. *Plate with hole domain*

	Direct Solver Time (seconds)					
h^{-1}	$p = 1$	$p = 2$	$p = 3$	$p = 4$	$p = 5$	$p = 6$
512	0.10	0.08	0.08	0.08	0.08	0.09
1024	0.57	0.52	0.44	0.40	0.40	0.44
2048	3.23	3.16	4.30	3.03	2.62	2.80
4096	18.62	18.39	31.18	26.59	17.78	21.11
8192	120.22	126.61	293.68	254.39	124.34	201.72

	ADI Iterations / Time (seconds)					
h^{-1}	$p = 1$	$p = 2$	$p = 3$	$p = 4$	$p = 5$	$p = 6$
512	29 / 0.20	28 / 0.20	29 / 0.23	30 / 0.25	31 / 0.29	32 / 0.30
1024	31 / 0.63	31 / 0.71	32 / 0.93	33 / 1.06	34 / 1.15	35 / 1.25
2048	34 / 3.57	34 / 4.35	35 / 5.63	36 / 6.19	37 / 7.17	37 / 7.96
4096	37 / 20.26	37 / 22.06	37 / 26.37	38 / 27.71	39 / 29.06	40 / 28.98
8192	40 / 68.40	39 / 95.30	40 / 88.72	41 / 94.27	42 / 104.97	43 / 108.82

TABLE 6.1

Square domain. Performance of the direct method (upper table) and of ADI (lower table)

no a posteriori stopping criterion is considered. Table 6.2 reports the relative error $\|e_J\|_M / \|e_0\|_M$ for all cases considered in Table 6.1: observe that in all cases, this value is below the prescribed tolerance 10^{-8} and at the same time, never smaller than $3 \cdot 10^{-9}$, showing that bound (4.10) is a tight estimate of the actual value.

We now turn to the first two problems with nontrivial geometry, namely the quarter of ring and the stretched square, and employ the direct method and ADI as preconditioners for CG (represented respectively by matrices \mathcal{P} and \mathcal{P}_J). For both problems, we set $\epsilon = 10^{-1}$ as tolerance for the ADI preconditioner. We remark that a slightly better performance could be obtained by an adaptive choice of ϵ , as described in [37, Chapter 3]. However, we did not implement this strategy.

To better judge the efficiency of the Sylvester-based approaches, we compare the results with those obtained when using a preconditioner based on the Incomplete Cholesky (IC) factorization (implemented by the MATLAB function `ichol`). To improve the performance of this approach, we considered some preliminary reorderings of \mathcal{A} , namely those implemented by the MATLAB functions `symrcm`, `symamd` and

h^{-1}	$p = 1$	$p = 2$	$p = 3$	$p = 4$	$p = 5$	$p = 6$
512	$3.0 \cdot 10^{-9}$	$7.0 \cdot 10^{-9}$	$6.8 \cdot 10^{-9}$	$6.4 \cdot 10^{-9}$	$6.7 \cdot 10^{-9}$	$6.7 \cdot 10^{-9}$
1024	$7.7 \cdot 10^{-9}$	$7.2 \cdot 10^{-9}$	$5.4 \cdot 10^{-9}$	$6.2 \cdot 10^{-9}$	$6.3 \cdot 10^{-9}$	$5.8 \cdot 10^{-9}$
2048	$7.5 \cdot 10^{-9}$	$6.0 \cdot 10^{-9}$	$4.9 \cdot 10^{-9}$	$6.0 \cdot 10^{-9}$	$5.1 \cdot 10^{-9}$	$9.7 \cdot 10^{-9}$
4096	$6.9 \cdot 10^{-9}$	$4.9 \cdot 10^{-9}$	$7.6 \cdot 10^{-9}$	$9.2 \cdot 10^{-9}$	$7.8 \cdot 10^{-9}$	$8.4 \cdot 10^{-9}$
8192	$6.1 \cdot 10^{-9}$	$8.2 \cdot 10^{-9}$	$7.5 \cdot 10^{-9}$	$9.3 \cdot 10^{-9}$	$7.9 \cdot 10^{-9}$	$8.2 \cdot 10^{-9}$

TABLE 6.2

ADI relative error $\|e_J\|_M / \|e_0\|_M$ at the final iteration for problems in Table 6.1

	CG + \mathcal{P} Iterations / Time (seconds)			
h^{-1}	$p = 2$	$p = 3$	$p = 4$	$p = 5$
128	25 / 0.04	25 / 0.05	25 / 0.07	25 / 0.10
256	25 / 0.16	25 / 0.22	25 / 0.29	25 / 0.36
512	26 / 0.74	26 / 0.92	26 / 1.24	26 / 1.73
1024	26 / 4.07	26 / 4.65	26 / 5.87	26 / 7.17

	CG + \mathcal{P}_J Iterations / Time (seconds)			
h^{-1}	$p = 2$	$p = 3$	$p = 4$	$p = 5$
128	25 (5) / 0.09	25 (5) / 0.13	25 (5) / 0.14	25 (5) / 0.18
256	26 (5) / 0.31	26 (5) / 0.40	26 (6) / 0.57	25 (6) / 0.70
512	27 (6) / 1.42	27 (6) / 1.85	26 (6) / 2.07	26 (6) / 2.72
1024	27 (6) / 5.53	27 (6) / 7.17	27 (7) / 9.91	27 (7) / 11.89

	CG + IC Iterations / Time (seconds)			
h^{-1}	$p = 2$	$p = 3$	$p = 4$	$p = 5$
128	65 / 0.14	49 / 0.18	40 / 0.25	33 / 0.32
256	130 / 1.06	98 / 1.30	80 / 1.81	65 / 2.04
512	264 / 8.43	198 / 9.99	160 / 12.01	128 / 14.23
1024	533 / 66.98	399 / 78.90	324 / 92.63	262 / 106.02

TABLE 6.3

Quarter of ring domain. Performance of CG preconditioned by the direct method (upper table), by ADI (middle table) and by Incomplete Cholesky (lower table).

`colperm`. The reported results refer to the `symrcm` reordering, which yielded the best performance. We remark that incomplete factorizations have been considered as preconditioners for IGA problems in [8], where the authors observed that this approach is quite robust w.r.t. p .

In Tables 6.3 and 6.4, we report the total computation time and the number of CG iterations for both problems; when ADI is used, we also report the number of iterations performed at each application of the preconditioner. Here and throughout, the computation time includes the time needed to setup the preconditioner. Note that the considered values of the mesh size are larger than in the square case. Indeed, while in the square case we need to store only the blocks M_1 , M_2 , K_1 and K_2 , in the presence of nontrivial geometry the whole matrix \mathcal{A} has to be stored, and this is unfeasible for our computer resources when h is too small. Below we report some comments on the numerical results for the two geometries: the quarter of ring and the stretched square.

- For both the ADI and the Bartels-Stewart preconditioners, the number of CG iterations is practically independent on p and slightly increases as the mesh is refined, but stays uniformly bounded according to Proposition 1. Moreover, in both approaches the computation times depend on p only mildly.
- The inexact application of \mathcal{P} via the ADI method does not significantly affects

	CG + \mathcal{P} Iterations / Time (seconds)				
h^{-1}	$p = 1$	$p = 2$	$p = 3$	$p = 4$	$p = 5$
128	58 / 0.07	61 / 0.08	62 / 0.12	61 / 0.16	61 / 0.21
256	64 / 0.27	66 / 0.35	66 / 0.48	66 / 0.69	66 / 0.86
512	69 / 1.40	70 / 1.78	69 / 2.21	69 / 3.05	69 / 4.28
1024	73 / 8.42	73 / 10.30	72 / 11.71	72 / 14.81	71 / 18.50

	CG + \mathcal{P}_J Iterations / Time (seconds)				
h^{-1}	$p = 1$	$p = 2$	$p = 3$	$p = 4$	$p = 5$
128	58 (5) / 0.20	61 (5) / 0.22	61 (5) / 0.27	61 (5) / 0.34	61 (5) / 0.42
256	65 (5) / 0.61	65 (5) / 0.72	65 (5) / 0.92	65 (6) / 1.38	66 (6) / 1.63
512	69 (6) / 2.92	70 (6) / 3.60	69 (6) / 4.43	69 (6) / 5.50	69 (6) / 7.19
1024	74 (6) / 12.30	73 (6) / 14.59	73 (6) / 18.70	72 (7) / 25.15	72 (7) / 31.07

	CG + IC Iterations / Time (seconds)				
h^{-1}	$p = 1$	$p = 2$	$p = 3$	$p = 4$	$p = 5$
128	50 / 0.07	38 / 0.08	26 / 0.10	22 / 0.15	20 / 0.23
256	102 / 0.50	88 / 0.72	53 / 0.75	44 / 1.03	38 / 1.40
512	213 / 4.06	232 / 7.26	115 / 6.13	89 / 7.10	76 / 9.26
1024	439 / 32.85	777 / 96.37	248 / 49.49	181 / 53.67	153 / 65.37

TABLE 6.4

Stretched square domain. Performance of CG preconditioned by the direct method (upper table), by ADI (middle table) and by Incomplete Cholesky (lower table).

the number of CG iterations. Moreover, the number of inner ADI iterations is roughly the same in all considered cases.

- The overall performance obtained with the direct method is slightly better than with ADI for all the considered discretization levels; if finer meshes are considered, ADI should eventually outperform the direct method.
- Interestingly, in the IC approach the number of CG iterations decreases for higher p . On the other hand, the CPU time still increases due to the greater computational cost of forming and applying the preconditioner.
- For small enough h , both the ADI and the Bartels-Stewart preconditioners yield better performance, in terms of CPU time, than the IC preconditioner.

Finally, we consider the problem on the plate with hole domain. As expected, the performance of the Sylvester-based preconditioners in this case is much worse than in the previous cases, and in particular the method is not robust neither w.r.t. h nor w.r.t. p . One can introduce modifications of \mathcal{P} that significantly improve the conditioning of the preconditioned system, however we postpone this investigation to a further work.

Interestingly, however, if we compare the results with the ones obtained with the IC preconditioner, we see that computation times are still in favor of the Bartels-Stewart preconditioner when h is small. In conclusion, even in most penalizing case among those considered, the proposed preconditioner is competitive with a standard one.

6.2. 3D experiments. As in the 2D case, we first consider a domain with trivial geometry, namely the unit cube $[0, 1]^3$, and then turn to more complicated domains. The first is a thick quarter of ring (figure 6.4); note this solid has a trivial geometry on the third direction. The second complicated domain is the solid of revolution obtained by the 2D quarter of ring (figure 6.5). Specifically, we performed a $\pi/2$ revolution around the axis having direction $(0, 1, 0)$ and passing through $(-1, -1, -1)$.

	CG + \mathcal{P} Iterations / Time (seconds)			
h^{-1}	$p = 2$	$p = 3$	$p = 4$	$p = 5$
128	125 / 0.16	155 / 0.26	186 / 0.45	216 / 0.72
256	191 / 1.10	238 / 1.53	277 / 2.62	319 / 3.76
512	279 / 5.51	345 / 10.02	406 / 15.08	446 / 25.32
1024	404 / 41.13	487 / 74.59	556 / 102.31	587 / 142.58

	CG + \mathcal{P}_J Iterations / Time (seconds)			
h^{-1}	$p = 2$	$p = 3$	$p = 4$	$p = 5$
128	199 (5) / 0.63	260 (5) / 1.00	321 (5) / 1.60	377 (6) / 2.58
256	348 (6) / 4.09	434 (6) / 6.25	522 (6) / 10.11	614 (6) / 15.12
512	580 (6) / 26.20	718 (6) / 41.23	851 (6) / 66.17	862 (7) / 97.59
1024	769 (7) / 183.51	968 (7) / 279.49	1173 (7) / 391.14	1348 (7) / 598.76

	CG + IC Iterations / Time (seconds)			
h^{-1}	$p = 2$	$p = 3$	$p = 4$	$p = 5$
128	92 / 0.16	55 / 0.18	45 / 0.25	38 / 0.35
256	180 / 1.30	114 / 1.41	90 / 1.75	73 / 2.12
512	354 / 10.59	253 / 12.26	193 / 13.92	151 / 15.84
1024	695 / 84.84	596 / 114.03	446 / 127.60	340 / 134.04

TABLE 6.5

Plate with hole domain. Performance of CG preconditioned by the direct method (upper table), by ADI (middle table) and by Incomplete Cholesky (lower table).

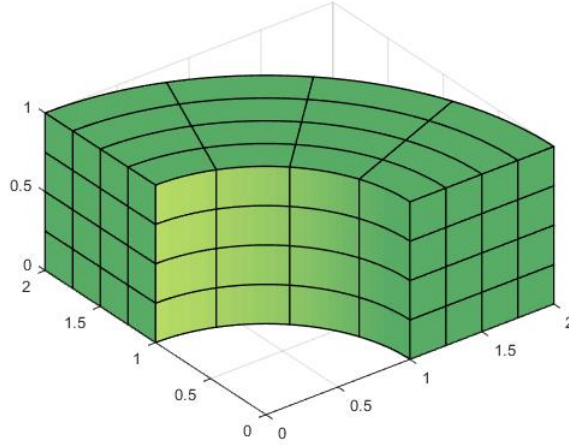
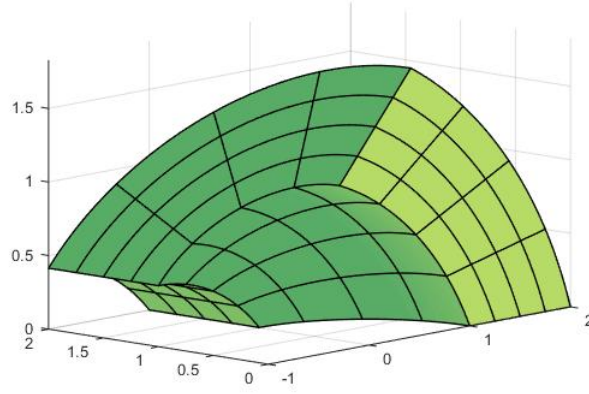


FIG. 6.4. Thick ring domain

We emphasize that here the geometry is nontrivial along all directions. In the cube case, we set $b = \text{randn}(n^3, 1)$ for computational ease, while in the other two cases b is the vector representing the function $f(x, y, z) = 2(x^2 - x) + 2(y^2 - y) + 2(z^2 - z)$. We again set K as the identity matrix in all cases.

We report in Table 6.6 the performances of the direct solver and of ADI relative to the cube domain. We can see that the computational time required by the direct solver is independent of the degree p . In fact, the timings look impressive and show the great efficiency of this approach. We emphasize that, on the finer discretization level, problems of more than one billion variables is solved in slightly more than one

FIG. 6.5. *Revolved ring domain*

	3D Direct Solver Time (seconds)					
h^{-1}	$p = 1$	$p = 2$	$p = 3$	$p = 4$	$p = 5$	$p = 6$
128	0.07	0.06	0.06	0.07	0.08	0.08
256	0.53	0.61	0.64	0.65	0.65	0.56
512	5.58	8.01	6.80	5.83	8.00	5.76
1024	66.79	68.46	67.30	66.38	66.60	63.86

	3D ADI Iterations / Time (seconds)					
h^{-1}	$p = 1$	$p = 2$	$p = 3$	$p = 4$	$p = 5$	$p = 6$
128	57 / 8.21	57 / 8.62	57 / 10.83	65 / 13.02	65 / 14.17	65 / 14.54
256	65 / 76.44	65 / 95.38	65 / 95.64	65 / 101.56	73 / 123.26	73 / 123.40
512	73 / 688.83	73 / 840.33	73 / 851.95	73 / 933.05	81 / 1106.50	81 / 890.45

TABLE 6.6

Cube domain. Performance of the direct solver (upper table) and of ADI (lower table). We did not run ADI on the finest level due to memory limitations.

minute (regardless of p). On the other hand, the ADI solver shows a considerably worse performance. Indeed, while the results confirm that this approach is quite robust w.r.t. h and p , the timings are always a couple of orders of magnitude greater than those obtained with the direct method. A comparison with Table 6.1 shows also that, as expected, the number of ADI iterations is higher than in the 2D case.

We now consider the problems with nontrivial geometries, where the two methods are used as preconditioners for CG. In the case of ADI, we again set $\epsilon = 10^{-1}$ for both problems. As in the 2D case, we also consider a standard Incomplete Cholesky (IC) preconditioner (no reordering is used in this case, as the resulting performance is better than when using the standard reorderings available in MATLAB).

In Table 6.7 we report the results for the thick quarter ring while in Table 6.8 we report the results for the revolved ring. The symbol “*” denotes the cases in which even assembling the system matrix \mathcal{A} was unfeasible due to memory limitations. From these results, we infer that most of the conclusions drawn for the 2D case still hold in the 3D case. In particular, both Sylvester-based preconditioners yield a better performance than the IC preconditioner, especially for small h .

	CG + \mathcal{P} Iterations / Time (seconds)				
h^{-1}	$p = 2$	$p = 3$	$p = 4$	$p = 5$	$p = 6$
32	26 / 0.21	26 / 0.42	26 / 0.83	26 / 1.63	26 / 2.84
64	27 / 1.46	27 / 3.36	27 / 7.41	27 / 13.44	27 / 22.95
128	28 / 12.74	28 / 30.30	28 / 60.14	*	*

	CG + \mathcal{P}_J Iterations / Time (seconds)				
h^{-1}	$p = 2$	$p = 3$	$p = 4$	$p = 5$	$p = 6$
32	26 (7) / 0.89	26 (7) / 1.12	26 (7) / 1.62	26 (7) / 2.53	27 (8) / 4.20
64	27 (7) / 5.38	27 (8) / 8.20	27 (8) / 12.69	27 (8) / 19.74	27 (8) / 28.98
128	28 (8) / 43.60	28 (8) / 66.12	28 (8) / 104.48	*	*

	CG + IC Iterations / Time (seconds)				
h^{-1}	$p = 2$	$p = 3$	$p = 4$	$p = 5$	$p = 6$
32	21 / 0.36	15 / 1.22	12 / 3.60	10 / 10.22	9 / 27.30
64	37 / 4.65	28 / 13.63	22 / 36.48	18 / 94.42	16 / 242.22
128	73 / 65.91	51 / 168.31	41 / 386.84	*	*

TABLE 6.7

Thick quarter of ring domain. Performance of CG preconditioned by the direct method (upper table), by ADI (middle table) and by Incomplete Cholesky (lower table).

	CG + \mathcal{P} Iterations / Time (seconds)				
h^{-1}	$p = 2$	$p = 3$	$p = 4$	$p = 5$	$p = 6$
32	40 / 0.30	41 / 0.62	41 / 1.25	42 / 2.61	42 / 4.47
64	44 / 2.16	44 / 5.21	45 / 11.15	45 / 21.83	45 / 36.60
128	47 / 21.99	47 / 56.58	47 / 113.42	*	*

	CG + \mathcal{P}_J Iterations / Time (seconds)				
h^{-1}	$p = 2$	$p = 3$	$p = 4$	$p = 5$	$p = 6$
32	40 (7) / 1.22	41 (7) / 1.62	41 (7) / 2.40	42 (7) / 3.87	42 (8) / 6.12
64	44 (7) / 7.47	44 (8) / 12.67	45 (8) / 19.17	45 (8) / 30.91	45 (8) / 47.35
128	47 (8) / 90.95	47 (8) / 128.85	47 (9) / 200.97	*	*

	CG + IC Iterations / Time (seconds)				
h^{-1}	$p = 2$	$p = 3$	$p = 4$	$p = 5$	$p = 6$
32	24 / 0.40	18 / 1.31	15 / 3.76	12 / 10.36	11 / 27.01
64	47 / 5.53	35 / 15.70	28 / 40.60	24 / 99.76	20 / 249.54
128	94 / 108.53	71 / 241.43	57 / 889.05	*	*

TABLE 6.8

Revolved quarter of ring domain. Performance of CG preconditioned by the direct method (upper table), by ADI (middle table) and by Incomplete Cholesky (lower table).

Somewhat surprisingly, however, the CPU times show a much stronger dependence on p than in the 2D case. Moreover, the performances of the ADI and Bartels-Stewart approaches are not as different as it was for the cube domain, where both methods were used as solvers. This is due to the cost of the residual computation in the outer CG iteration (a sparse matrix-vector product, costing $O(p^3 n^3)$ FLOPs). This step represents now a significant computational effort in the overall CG performance. In fact, our numerical experience shows that the 3D direct method is so efficient that its cost is often negligible w.r.t. to the cost of the residual computation. This effect is clearly shown in Table 6.9, where we report the percentage of time spent in the application of the preconditioner when compared with the overall time

h^{-1}	$p = 2$	$p = 3$	$p = 4$	$p = 5$	$p = 6$
32	24.43	12.40	6.52	4.15	2.66
64	19.60	9.10	3.78	2.21	1.24
128	15.58	7.00	3.73	*	*

TABLE 6.9

Percentage of time spent in the application of the 3D Bartels-Stewart preconditioner with respect to the overall CG time. Revolved ring domain.

of CG, in the case of the revolved ring domain.

7. Conclusions. In this work we have analysed and tested the use of fast solvers for Sylvester-like equations as preconditioners for isogeometric discretizations.

We considered here a Poisson problem on a single-patch domain, and we focused on the k -method, i.e., splines with maximal smoothness. The considered preconditioner \mathcal{P} is robust w.r.t. h and p , and we have compared two popular methods for its application. We found that the Bartels-Stewart direct solver, especially in 3D, is by far more effective than the ADI iterative solver. Both approaches easily outperform a simple-minded incomplete Cholesky preconditioner.

Our conclusion is that the use of a Bartels-Stewart solver is, likely, the best possible choice to compute the action of the operator \mathcal{P}^{-1} . This is, then, a very promising preconditioner stage in an iterative solver for isogeometric discretizations. In a forthcoming paper we will further study the role of the geometry parametrization on the performance of the approach based on Sylvester equation solvers, and propose possible strategies to improve it.

Acknowledgments. The authors would like to thank Valeria Simoncini for fruitful discussions on the topics of the paper. The authors were partially supported by the European Research Council through the FP7 Ideas Consolodator Grant *HIGEOM*. This support is gratefully acknowledged.

REFERENCES

- [1] J. BALLANI AND L. GRASEDYCK, *A projection method to solve linear systems in tensor format*, Numerical Linear Algebra with Applications, 20 (2013), pp. 27–43.
- [2] R. H. BARTELS AND G. W. STEWART, *Solution of the matrix equation $AX + XB = C$* , Communications of the ACM, 15 (1972), pp. 820–826.
- [3] Y. BAZILEVS, C. MICHLER, V. M. CALO, AND T. J. R. HUGHES, *Isogeometric variational multiscale modeling of wall-bounded turbulent flows with weakly enforced boundary conditions on unstretched meshes*, Computer Methods in Applied Mechanics and Engineering, 199 (2010), pp. 780–790.
- [4] L. BEIRAO DA VEIGA, A. BUFFA, G. SANGALLI, AND R. VÁZQUEZ, *Mathematical analysis of variational isogeometric methods*, Acta Numerica, 23 (2014), pp. 157–287.
- [5] L. BEIRÃO DA VEIGA, D. CHO, L. F. PAVARINO, AND S. SCACCHI, *Bddc preconditioners for isogeometric analysis*, Mathematical Models and Methods in Applied Sciences, 23 (2013), pp. 1099–1142.
- [6] M. BERCOVIER AND I. SOLOVEICHNIK, *Overlapping non matching meshes domain decomposition method in isogeometric analysis*, arXiv preprint arXiv:1502.03756, (2015).
- [7] A. BUFFA, H. HARBRECHT, A. KUNOTH, AND G. SANGALLI, *Bpx-preconditioning for isogeometric analysis*, Computer Methods in Applied Mechanics and Engineering, 265 (2013), pp. 63–70.
- [8] N. COLLIER, L. DALCIN, D. PARDO, AND V. M. CALO, *The cost of continuity: performance of iterative solvers on isogeometric finite elements*, SIAM Journal on Scientific Computing, 35 (2013), pp. A767–A784.

- [9] N. COLLIER, D. PARDO, L. DALCIN, M. PASZYNSKI, AND V. M. CALO, *The cost of continuity: a study of the performance of isogeometric finite elements using direct solvers*, Computer Methods in Applied Mechanics and Engineering, 213 (2012), pp. 353–361.
- [10] J. A. COTTRELL, T. J. R. HUGHES, AND Y. BAZILEVS, *Isogeometric analysis: toward integration of CAD and FEA*, John Wiley & Sons, 2009.
- [11] J. A. COTTRELL, T. J. R. HUGHES, AND A. REALI, *Studies of refinement and continuity in isogeometric structural analysis*, Computer methods in applied mechanics and engineering, 196 (2007), pp. 4160–4183.
- [12] L. BEIRAO DA VEIGA, D. CHO, LUCA F. PAVARINO, AND SIMONE SCACCHI, *Overlapping schwarz methods for isogeometric analysis*, SIAM Journal on Numerical Analysis, 50 (2012), pp. 1394–1416.
- [13] C. DE FALCO, A. REALI, AND R. VÁZQUEZ, *Geopdes: a research tool for isogeometric analysis of pdes*, Advances in Engineering Software, 42 (2011), pp. 1020–1034.
- [14] J. W. DEMMEL, *Applied numerical linear algebra*, Siam, 1997.
- [15] M. DONATELLI, C. GARONI, C. MANNI, S. SERRA-CAPIZZANO, AND H. SPELEERS, *Robust and optimal multi-iterative techniques for iga galerkin linear systems*, Computer Methods in Applied Mechanics and Engineering, 284 (2015), pp. 230–264.
- [16] J. DOUGLAS, *Alternating direction methods for three space variables*, Numerische Mathematik, 4 (1962), pp. 41–63.
- [17] N. S. ELLNER AND E. L. WACHSPRESS, *Alternating direction implicit iteration for systems with complex spectra*, SIAM journal on numerical analysis, 28 (1991), pp. 859–870.
- [18] K. P. S. GAHALAUT, J. K. KRAUS, AND S. K. TOMAR, *Multigrid methods for isogeometric discretization*, Computer methods in applied mechanics and engineering, 253 (2013), pp. 413–425.
- [19] L. GAO, *Kronecker Products on Preconditioning*, PhD thesis, King Abdullah University of Science and Technology, 2013.
- [20] G. H. GOLUB AND C. F. VAN LOAN, *Matrix computations*, JHU Press, 2012.
- [21] L. GRASEDYCK, *Existence and computation of low kronecker-rank approximations for large linear systems of tensor product structure*, Computing, 72 (2004), pp. 247–265.
- [22] C. HOFREITHER, S. TAKACS, AND W. ZULEHNER, *A robust multigrid method for isogeometric analysis using boundary correction*, Tech. Report 33, NFN, 2015.
- [23] T. J. R. HUGHES, J. A. COTTRELL, AND Y. BAZILEVS, *Isogeometric analysis: CAD, finite elements, NURBS, exact geometry and mesh refinement*, Comput. Methods Appl. Mech. Engrg., 194 (2005), pp. 4135–4195.
- [24] T. G. KOLDA AND B. W. BADER, *Tensor decompositions and applications*, SIAM review, 51 (2009), pp. 455–500.
- [25] D. KRESSNER AND C. TOBLER, *Krylov subspace methods for linear systems with tensor product structure*, SIAM journal on matrix analysis and applications, 31 (2010), pp. 1688–1714.
- [26] B. W. LI, S. TIAN, Y. S. SUN, AND Z. M. HU, *Schur-decomposition for 3d matrix equations and its application in solving radiative discrete ordinates equations discretized by chebyshev collocation spectral method*, Journal of Computational Physics, 229 (2010), pp. 1198–1212.
- [27] A. LU AND E. L. WACHSPRESS, *Solution of lyapunov equations by alternating direction implicit iteration*, Computers & Mathematics with Applications, 21 (1991), pp. 43–58.
- [28] R. E. LYNCH, J. R. RICE, AND D. H. THOMAS, *Direct solution of partial difference equations by tensor product methods*, Numerische Mathematik, 6 (1964), pp. 185–199.
- [29] D. PALITTA AND V. SIMONCINI, *Matrix-equation-based strategies for convection-diffusion equations*, arXiv preprint arXiv:1501.02920, (2015).
- [30] D. W. PEACEMAN AND H. H. RACHFORD, *The numerical solution of parabolic and elliptic differential equations*, Journal of the Society for Industrial & Applied Mathematics, 3 (1955), pp. 28–41.
- [31] T. PENZL, *A cyclic low-rank smith method for large sparse lyapunov equations*, SIAM Journal on Scientific Computing, 21 (1999), pp. 1401–1418.
- [32] V. SIMONCINI, *Computational methods for linear matrix equations*, to appear on SIAM Review, (2013).
- [33] L. SORBER, M. VAN BAREL, AND L. DE LATHAUWER, *Tensorlab v2. 0*, Available online, URL: www.tensorlab.net, (2014).
- [34] E. L. WACHSPRESS, *Optimum alternating-direction-implicit iteration parameters for a model problem*, Journal of the Society for Industrial & Applied Mathematics, 10 (1962), pp. 339–350.
- [35] ———, *Extended application of alternating direction implicit iteration model problem theory*, Journal of the Society for Industrial & Applied Mathematics, 11 (1963), pp. 994–1016.
- [36] ———, *Three-variable alternating-direction-implicit iteration*, Computers & Mathematics with

- Applications, 27 (1994), pp. 1–7.
- [37] ———, *The ADI model problem*, Springer, 2013.